Searching for solvent cavities via electron photodetachment: The ultrafast charge-transfer-to-solvent (CTTS) dynamics of sodide in a series of ether solvents

Molly C. Larsen* and Benjamin J. Schwartz†

Department of Chemistry and Biochemistry,

University of California, Los Angeles, Los Angeles, CA 90095-1569

(Dated: September 18, 2009)

It was recently predicted by simulations and confirmed by neutron diffraction experiments that the structure of liquid tetrahydrofuran (THF) contains cavities. The cavities can be quite large and have a net positive electrostatic potential, so they can serve as pre-existing traps for excess electrons created via photodetachment from various solutes. In this paper, we use electron photodetachment via charge-transfer-to-solvent (CTTS) excitation of sodide (Na^-) to probe for the presence of pre-existing cavities in a series of ether solvents: THF, diethyl ether (DEE), 1,2-dimethoxyethane (DME) and diglyme (DG). We find that electrons photodetached from sodide appear after a time delay with their equilibrium spectrum in all of these solvents, suggesting that the entire series of ethers contains pre-existing solvent cavities. We then use the variation in electron recombination dynamics with CTTS excitation wavelength to probe the nature of the cavities in the different ethers. We find that the cavities that form the deepest electron traps turn on at about the same energy in all four ether solvents investigated, but that the density of cavities is lower in DG and DME than in THF. We also examine the dynamics of the neutral sodium species that remains following CTTS photodetachment of an electron from sodide. We find that the reaction of the initially-created gas-phase-like Na atom to form a (Na^+, e^-) tight-contact pair occurs at essentially the same rate in all four ether solvents, indicating that only local solvent motions and not bulk solvent rearrangements are what is responsible for driving the partial ejection of the remaining Na valence electron.

I. INTRODUCTION

Although experiments that measure solvation dynamics, the relaxation of a solvent around a newly-excited solute, are common,[1–9] we still have relatively little understanding of the connections between the intrinsic structure of a solvent and chemical reaction dynamics. For example, it was recently predicted by molecular dynamics simulations[10,11] and verified by neutron diffraction experiments[12] that the solvent structure of liquid tetrahydrofuran (THF) is characterized by electropositive voids: the natural structure of liquid THF contains cavities that can be larger than an entire solvent molecule, and the electrostatic potential in these cavities is favorable for solvating the excess electrons that are created via anion photodetachment in this solvent. Mixed quantum/classical simulations have suggested that the high-lying excited states of anions dissolved in liquid THF are disjoint:[11,13] excited electrons can have density in the multiple solvent cavities, including cavities far from the one that houses the ground-state anion.

The presence of such cavities and the disjoint electronic states that they support has important consequences for electron photodetachment in solvents like THF.[14–17] For example, in the red-edge excitation of anions such as I^- in THF, coupling of the local charge-transfer-to-solvent (CTTS) excited state to solvent-supported disjoint states with similar energies leads to photoejection of electrons to significant distances ($\sim$6 nm) from the parent anion.[16] Another experimental signature of cavities is that the detached electrons produced after exciting nearly any anion in liquid THF — I^-,[17] Na^-,[14] K^-[18] or even the solvated electron itself[19] — appear after a $\sim$0.5-ps time delay with their equilibrium spectrum.[20] This indicates that excited electrons relax directly into pre-existing solvent traps from the initially-prepared solvent-supported excited state.[11] Finally, the presence of cavities allows for photoinduced charge relocalization: photoexcitation has been used to move electrons through liquid THF to enhance recombination with both neutral[21–23] and positively-charged[16] solutes that lie a significant distance away from the electron's original location, results that match well with cavity-induced relocalization behavior seen in quantum simulations.[11]

Although solvent cavities play a direct role in electron photodetachment reactions, characterizing such cavities, and indeed even probing their existence, is challenging. For example, many groups have performed molecular dynamics simulations of liquid THF[24–28] and other ethers[29–31] over the years, but the presence of cavities in such simulations was noticed only

fairly recently.[10,11] In addition, Fourkas and co-workers used the optical Kerr effect to examine the low-frequency motions of a series of organic solvents, but they were unable to find any obvious experimental signatures that could be associated with the presence of cavities.[32] Neutron diffraction is clearly the best way to investigate the presence of solvent cavities,[12,33] but it does not offer a high-throughput way to search for the presence of cavities in multiple solvents or solvent mixtures. Thus, in this paper, we investigate whether or not a series of ether solvents contain cavities by measuring the ultrafast dynamics of electrons created by photodetachment: we take advantage of the fact that charge-transfer-to-solvent (CTTS) excitation of anions in solvents that do not contain cavities, such as water and alcohols, leads to prompt electron detachment followed by slower electron solvation,[34–38] in contrast to the delayed appearance and complete lack of dynamic solvation associated with CTTS photodetachment in cavity-containing liquid THF.[14,15,39,40] We have argued in previous work that the signatures of CTTS electron detachment from from Na^- (sodide) are similar enough in liquid THF and liquid diethyl ether (DEE) that DEE is likely a cavity-containing solvent akin to liquid THF.[18] In this work, we extend these preliminary studies to examine the CTTS electron detachment dynamics of sodide in 1,2-dimethoxyethane (DME) and diglyme (DG), which with DEE and THF comprise a series of ethers (see Figure 1 for the chemical structures of these solvents). We chose this series so that we could directly investigate, without varying the functional groups or basic properties of the solvent, whether or not cavities exist in these solvents, and if they do exist, how the ether chain length controls the relative energies of the disjoint electronic excited states that the cavities support.

Our choice to search for cavities using the CTTS dynamics of sodide is predicated on the fact that the electron detachment dynamics of Na^- in liquid THF has been extensively studied in previous work by both our group[14,15,19,21,22,39,41–43] and others,[44–46] so that the Na^-/THF system serves as an excellent reference point for understanding the relationship between CTTS dynamics and the presence of solvent cavities in other solvents. Photoexcitation of the sodide CTTS transition in liquid THF is known to produce solvated electrons and neutral sodium atoms:[47,48]

$$Na^- \xrightarrow{\text{CTTS}} Na^0 + e^- \tag{1}$$

where e^- is the solvated electron and Na^0 is a neutral sodium atom. As mentioned above, our previous ultrafast pump-probe experiments[19,21,22,40–43,49] have shown that the solvated electrons produced following CTTS excitation of Na^- in THF appear with their equilibrium

spectrum after a ∼0.5-ps time delay, the signature that we have argued is the time scale for an excited electron to access the lowest disjoint state before being ejected into a pre-existing solvent cavity.[14,17,18]

Our previous work also found that the percentage of electrons that undergo geminate recombination with their Na^0 partners within the first few ps following excitation was dependent on the CTTS excitation wavelength.[41] We have argued that this wavelength dependence results from coupling between "bright" CTTS excited states that are localized in the anion's solvent cavity and the naturally-occurring disjoint states supported by solvent cavities that can be far from the anion.[10,11,14,17,18] Thus, the amount of recombination in the first few ps following CTTS excitation of Na^- provides a means to gauge the density of the cavity-supported disjoint states: the higher the density of solvent-supported disjoint states, the greater their coupling to the CTTS bright states. The more likely an excited electron is to couple into the disjoint states, the more likely it is to be ejected far from the parent anion and thus the less likely it is to undergo geminate recombination in the first few ps. One of our goals in this work is to use the wavelength dependence of geminate recombination following CTTS excitation of Na^- to compare the density of disjoint excited states supported by any naturally-occurring cavities in the different ether solvents.

Another goal of this work is to study how the dynamics of the neutral atomic sodium species left behind after electron photodetachment depend on the solvent. Both we[15,19,21,22,39–43,49,50] and others[44–46] have studied the ultrafast absorption dynamics of this atomic species in THF and found some surprisingly complex dynamics. Immediately following CTTS excitation, the initially-created neutral sodium atom (Na^{0*}) absorbs near 600 nm, the position of the gas-phase Na D-line, suggesting that this initial species is gas-phase-like and only weakly interacts with the surrounding solvent. After some initial solvent relaxation, the 600-nm absorption decays and new absorption grows in concomitantly at redder wavelengths, with an isosbestic point indicating two-state kinetics.[14] We have assigned these kinetics to a partial electron-transfer reaction of the relaxed sodium atom (Na^0) to form a sodium cation:solvated electron tight-contact pair, (Na^+, e^-):[14]

$$Na^{0*} \xrightarrow[\text{Solv.}]{\sim 200 \text{ fs}} Na^0 \xrightarrow[\text{Rxn.}]{\sim 750 \text{ fs}} (Na^+, e^-)^* \xrightarrow[\text{Solv.}]{\sim 5-10 \text{ ps}} (Na^+, e^-) \tag{2}$$

where "Solv." indicates a solvation process, "Rxn." indicates a chemical reaction and * denotes a species that is not equilibrated with the solvent. We note that in the final step,

we have argued that the solvation dynamics that bring the newly-created tight-contact pair (TCP) into equilibrium with the THF solvent fall outside of the linear response regime.[51] In the experiments presented below, we examine the generality of Eq. 2 in describing the mechanism for Na atom relaxation following CTTS excitation of Na^- in our series of ethers and investigate how each of the time scales in Eq. 2 are affected by the choice of solvent.

The rest of this paper proceeds as follows. In Section II, we present the experimental methods used in this study. Section III summarizes some of the bulk properties of our series of ether solvents and discusses the steady-state absorption spectra of the sodide reactant and solvated electron and neutral sodium products in these solvents. Section IV then presents the results of experiments that monitor the dynamics of the electron ejected following CTTS excitation of Na^- in our ether solvent series. In Section V, we examine the dynamics of the neutral atomic sodium species that remains following photodetachment of the CTTS electron from Na^- in each of our ether solvents. Finally, we present a summary and our conclusions in Section VI. with a discussion comparing how the cavity-containing solvent structure of the ethers leads to different CTTS electron photodetachment dynamics than what is observed in non-cavity-containing solvents such was water and alcohols.

II. EXPERIMENTAL

For all of the experiments reported here, we used solvents purchased from Sigma-Aldrich. We distilled THF over sodium and potassium and stored the distilled liquid in a glove box until use. We also stored and handled anhydrous DEE (>99%), DME (>99.5%) and DG (>99.5%) in a glove box, and otherwise used these solvents as received without further purification. We prepared our samples of sodide in THF using a technique described previously,[14] which was based on the original method used by Dye.[52–56] Briefly, we synthesized Na^- in THF by dissolving a small amount sodium and potassium metal into a ∼1:1000 15-crown-5 ether:THF mixture that had been placed in a 1-mm air-tight spectrophotometer cell and sonicating until the characteristic dark blue color of sodide appeared. Our preparation of sodide in DEE was similar, except that a small amount of 18-crown-6 ether was needed to help initiate the dissolution.[40] As described in detail previously,[18] because sodide and potasside have similar stabilities in DEE, we took care to ensure that all the DEE samples we prepared were free from potasside contamination.

We prepared sodide samples in DME and DG using a technique similar to that in THF, except that crown ether was not needed to initiate dissolution of the metal. We found it challenging to prepare samples of sodide in DME with concentrations high enough for some experiments, so when needed, we added a small amount of 15-crown-5 ether to aid metal dissolution in these solutions. We verified, however, that the transient absorption dynamics we measured in DME were the same whether or not the crown ether was used in the sample preparation. On the contrary, it was quite easy to prepare highly-concentrated samples of sodide in DG even in the absence of crown ether. In fact, the ease of metal dissolution in DG led to samples with an optical density so high that it was difficult to measure the UV-Visible absorption spectrum of the anion and to perform some transient bleach experiments. To remedy this, we prepared samples of sodide in DG in 0.5-mm air-tight spectrophotometer cells, and we let the samples sit at room temperature until the optical density decreased enough to make UV-Visible absorption and transient bleach experiments feasible.[57] Once we were able to take the absorption spectrum, we found no spectroscopic evidence for the presence of potasside, the solvated electron, or the solvated neutral potassium or sodium species at equilibrium. We also note that some of the Na^-/DME samples, particularly those that were freshly prepared, were unstable in the presence of laser radiation. In this case, we rastered these samples in a direction perpendicular to the excitation and probe beams using a computer-controlled translation stage to ensure that a fresh sample was being examined with every few laser shots, and we verified that the transient absorption dynamics we measured in this solvent did not depend on whether or not the sample was rastered or the rate of rastering. Most samples lasted for several days when stored in the dark at ~ -20 °C when not in use; all of the data were collected on samples at room temperature.

The details of our pump-probe apparatus have been described elsewhere.[58] In brief, we use an amplified Ti:Sapphire laser that produces light pulses of ~120-fs duration with ~800 μJ of energy centered at ~785 nm at a 1 kHz repetition rate. A portion of the fundamental light is directed into an optical parametric amplifier (OPA) where it is down-converted into near-IR signal and mid-IR idler beams. The remainder of the fundamental light is then used either directly as the excitation beam or doubled in a beta barium borate (BBO) crystal to make light at 395 nm. For experiments probing near either 1100 nm or 2000 nm, the signal or idler light from the OPA was used directly as the probe beam, respectively. 580-nm probe light was produced by sum-frequency mixing the idler beam with some of the leftover

fundamental beam in another BBO crystal. For all of the experiments, either the pump or the probe beam was directed onto a computer-controlled translation stage so that the delay between the pump and probe beam could be varied. Probe pulses at visible, near-IR or mid-IR wavelengths were detected on silicon, Indium-Gallium-Arsenide, or Indium-Arsenide photodiodes, respectively. For all wavelength ranges, part of the probe beam was directed to an identical reference detector so that variations in the laser intensity could be normalized. We chopped the pump beam so that we could normalize the recorded signals by comparing the ratio of the signal and reference probe beams with the pump impinging on the sample to that when the pump beam was blocked. The electrical signal from each photodetector was directed into a fast gated A-to-D converter so that laser shots outside of preset intensity bounds could be rejected on the fly and that the data could be double-normalized on a shot-by-shot basis. All of the pump-probe transients shown in this paper were collected with the relative polarization of the pump and probe beams set at the magic angle, 54.7°. The error bars in each data set presented below represent 95% confidence-limit intervals determined from averaging multiple pump-probe data sets collected by scanning the delay stage back and forth in a single experiment. All the experiments were done at several pump intensities to ensure that we were safely in the linear excitation regime.[42]

III. BACKGROUND: THE SPECTROSCOPY OF SODIDE AND ITS PHOTOPRODUCTS IN ETHER SOLVENTS

Although the aim of this study was to investigate the pump/probe dynamics of Na^- in a series of ether solvents that have similar bulk properties but different chain lengths, no series of solvents allows for precise control over any particular bulk property. This is true for the ether solvent series we have elected to use here. Table I summarizes several of the bulk properties of the solvents studied here, including the index of refraction (n),[59] the static dielectric constant (ϵ/ϵ_0),[60,61,62] and the viscosity (η).[63,64] Table I also includes the solvent polarity as measured by the solvatochromatic shift of the absorption spectrum of the dye penta-*tert*-butyl pyridinium N-phenolate betaine in solution, the E_T^N value.[65,66] The table shows that DEE provides the least polar environment of the solvents studied, although the E_T^N values and static dielectric constants of all the solvents are fairly similar. The similar polarity of these solvents is perhaps not surprising given that molecular dynamics

	n[a]	η (mPa s)	ϵ/ϵ_0	E_T^{Nf}
THF	1.4070	0.456[b]	7.47[d]	0.207
DEE	1.3555	0.224[b]	4.42[d]	0.117
DME	1.3739	0.420[c]	7.2[e]	0.231
DG	1.4097	1.003[c]	??	0.244

TABLE I: Bulk properties of the ether solvents used in this study: n is the index of refraction, η is the viscosity, ϵ/ϵ_0 is the static dielectric constant, and E_T^N is a measure of the solvatochromatic shift in the absorption spectrum of penta-*tert*-butyl pyridinium N-phenolate betaine in solution (see text). *a*: Reference 59. *b*: Reference 63. *c*: Reference 64. *d*: Reference 60. *e*: Reference 61. *f*: Reference 65. To the best of our knowledge the dielectric constant for DG has not been measured.

simulations show that $CH_3(CH_2OCH_2)_nH$ with $n = 1$ and 2 give nearly identical solvent structures around both neutral and cationic solutes.[29] Thus, we expect the local solvation stucture to vary minimally among the straight-chain ethers, so that the only significant variation in bulk property across our solvent series is the factor of $\sim$4 variation in viscosity.

The various curves in the upper panel of Figure 2 show the UV-Visible absorption spectrum of sodide in our series of ether solvents as measured in our laboratory. Since we could not independently determine the concentration of the sodide samples, we have assumed that the maximum extinction coefficient of the sodide CTTS transition was the same in all of the solvents as in THF.[47] For reference, the dashed grey curve in this figure shows the spectrum of sodide in THF taken from Gaussian-Lorentzian fit parameters in the literature.[47,67] The figure shows that the absorption spectra of sodide in THF, DME, and DG all have essentially the same shape and an almost identical maximum wavelength. The absorption spectrum of sodide in DEE and THF appear to be slightly broader than that in the other solvents, which we have argued previously is likely the result of either a small amount of potasside contamination or scattering from metal oxide particles in the DEE samples.[18,40]

The various curves in the lower panel of Figure 2 show the absorption spectrum of the solvated electron in THF, DEE, DME and DG, taken from fit parameters given in the literature.[68] The spectrum of the equilibrium neutral sodium species in liquid THF, also taken from pulse radiolysis experiments in the literature,[47] is shown as the purple dashed curve in this figure. This spectrum has been assigned on the basis of both quan-

tum simulations[69] and experiments[14,44,47,70–72] as arising from a (Na^+, e^-) tight-contact pair (TCP), a species in which the electron is partially on the sodium cation and partially in the solvent. The partial valence interaction of the electron with the sodium cation in the TCP gives rise to an absorption spectrum that peaks near 900 nm, part way between that of a gas-phase sodium atom and a solvated electron.[69]

We note that somewhat surprisingly, there is no evidence in the literature for the presence of (Na^+, e^-) tight-contact pairs at equilibrium in DEE; instead, pulse radiolysis of sodium cations in DEE produces a species with an absorption maximum at ∼700 nm, suggestive of the formation of sodide.[73] However, previous ultrafast experiments[18,40] (and this study) suggest that (Na^+, e^-) TCPs do form in liquid DEE on sub-ns time scales. We also note that pulse radiolysis experiments suggest that the interactions between sodium cations and electrons in both DME and DG are more complex than what is observed in THF.[74,75] In both DME and DG, the room-temperature solvated neutral sodium species exists in two forms as an equilibrium between a tight-contact pair, which absorbs near 900 nm as in THF, and a loose-contact pair (LCP), which has an absorption spectrum similar in shape to that of the solvated electron but with its spectral maximum blue-shifted to near 1600 nm.[74,75] Thus, the interaction between sodium cations and electrons varies significantly across our series of ethers: in liquid THF, only the tight-contact pair is observed at equilibrium at room temperature,[76] whereas both the TCP and LCP appear in equilibrium with each other in DME and DG, and neither is observed at equilibrium in DEE.

IV. THE DYNAMICS OF ELECTRON PHOTODETACHMENT FROM SODIDE IN DIFFERENT ETHER SOLVENTS

In this section we describe the results of experiments in which we excite the sodide CTTS band in our different ether solvents and probe the dynamics of the photodetached electrons in the spectral region near 2000 nm. Since we find the spectral signatures associated with the presence of cavities in all of our ether solvents, we then study the electron recombination dynamics as the CTTS excitation wavelength is varied,[41] allowing us to probe how the density of the cavity-supported disjoint states varies in each of these solvents.

A. Evidence for Cavities in Ethers Based on the Dynamics of Electron Photodetachment

In Figure 3 we show the results of pump-probe experiments examining the dynamics of the photodetached electrons created following CTTS excitation of sodide in DME (left panels) and DG (right panels); the sodide CTTS band is excited both at 785 nm (bottom panels) and at 395 nm (top panels), and the dynamics of the detached electron are probed at various wavelengths between ∼1735 nm and ∼2450 nm. In each panel, there is a ∼0.5-ps delay in the appearance of electron's transient absorption, and the dynamics at every probe wavelength are identical within the experimental signal-to-noise: there is no evidence for any dynamic solvation once the electron is formed. This indicates that the photodetached electrons are rapidly localized into pre-existing traps, presumably naturally-occuring solvent cavities. Thus, the fact that photodetached solvated electrons in DME and DG appear after a delay with their equilibrium absorption spectrum, as seen previously in THF and DEE, suggests that all of the ethers are cavity-containing solvents.[10–12,14,17,18] We have argued that that non-adiabatic relaxation through disjoint states supported by pre-existing cavities is the primary reason for the delayed appearance time of photodetached electrons in liquid THF.[14,16–18] The fact that the time scale for electron appearance is similar across all the ethers reinforces this idea: if significant solvent rearrangement were necessary to drive the detachment process, we would have expected the time scale for electron appearance to get slower in longer-chained ethers, as is observed following CTTS electron detachment from iodide in longer-chained alcohols.[38] The fact that the appearance time is the same in these very different solvents is strong evidence that only local solvent motions, not significant solvent rearrangements, are needed to foster detachment of an excited electron.

Another interesting aspect to the data shown in Figure 3 is that there is no evidence for the formation of sodium cation:solvated electron loose-contact pairs, as was seen in pulse radiolysis experiments in both DME and DG.[74,75] This is based on the fact that the transient absorption dynamics we measured in DME and DG were independent of probe wavelength with 395-nm excitation for the probe wavelengths shown in Fig. 3 out to ∼30 ps (not shown). Since any dynamics involved in the formation of an LCP from the initially-created neutral sodium atom would be quite different from the dynamics of the detached electron (Eqs. 1 and 2) and since LCPs and solvated electrons have slightly different but strongly overlapping

absorption spectra, we would have expected to see different dynamics at the different probe wavelengths (even in the absence of solvation of the detached electrons) if any of the neutral sodium species became LCPs. The data in Figure 3 show that this is not the case. It is unlikely that we missed any spectral signatures of LCP formation in these experiments since we were able to observe the formation of a small fraction of LCPs in previous work examining the photodetachment of electrons from tetrabutylammmonium iodide in liquid THF.[16] Thus, we conclude that the equilibrium sodium cation:solvated electron loose-contact pair does not form in DME or DG on the time scales examined in this experiment.

Figure 4 compares the transient absorption dynamics of the detached electrons following both 395-nm (left panel) and 785-nm (right panel) CTTS excitation of sodide in all of the solvents shown in Fig. 1. In addition to the fact that the appearance time of the electron is nearly identical in each of the solvents, the data in Fig. 4 show that the faster, ∼1-ps time scale for geminate recombination of the detached electrons with their neutral sodium partners is also nearly identical in all the solvents studied (except for DEE, where the slightly slower time scale for recombination had been previously observed[18,40]). The fact that this recombination time scale is so similar in these very different solvents is strong support that this recombination originates from a population of the electrons trapped in the same cavity as the neutral Na species; we have referred to these types of electrons as residing in sodium atom:solvated electron 'immediate contact pairs'.[19,21,22,40–43,49] If diffusion of the electron or any significant amount of solvent reorganization was required for this recombination to occur, we should have seen the slowest back electron transfer dynamics in DG. The fact that we actually see the slowest dynamics in DEE, the least viscous solvent in our series, indicates that wavefunction overlap or some other factor that depends only weakly on solvent is what drives the fast geminate recombination of the detached electrons with their neutral partners.

B. Mapping the Density of Solvent-Cavity-Supported Disjoint States Using Electron Recombination Dynamics

It has been shown for sodide in several solvents[18,40] that the fraction of detached electrons that undergo rapid geminate recombination decreases as the CTTS excitation energy increases. This can be understood on the basis of simulations, which found that the density of cavity-supported electronic states increases with energy.[11,13] This suggests that excitation

to higher-lying bound CTTS states increases the likelihood of coupling to cavity-supported disjoint states and thus decreases the number of electrons that remain close enough to their parent atoms to undergo rapid recombination. Thus, the excitation wavelength dependence of the geminate recombination dynamics of CTTS electrons photodetached from sodide provides a means to map out the density of the disjoint electronic states supported by the naturally-occuring cavities in our series of ether solvents. The fact that the CTTS absorption spectrum of sodide is essentially identical across our series of ether solvents (Figure 2) allows us to meaningfully compare the electron recombination dynamics at a given excitation wavelength and thus infer the density of solvent-supported cavities in the different solvents.

Figure 5 shows the dynamics of the photodetached electrons following CTTS excitation of sodide in THF (green curves), DME (blue curves) and DG (red curves) at the intermediate excitation wavelengths of 490 nm (top panel), 575 nm (middle panel) and 635 nm (bottom panel).[77] The figure shows that the general trend of an increasing fraction of long-lived electrons with increasing excitation energy that we observed previously in THF[41] holds across all the ether solvents. What is perhaps more surprising, however, is that the fraction of long-lived electrons produced at intermediate excitation wavelengths is *different* across our solvent series even though we saw above in Figure 4 that this fraction was the same in all the solvents following excitation at both 395 nm and 785 nm.

To better compare the different recombination dynamics at different excitation wavelengths in the different ether solvents, Figure 6 shows a summary of the fraction of long-lived electrons, calculated as the ratio of the magnitude of the electron's absorption signal averaged at 7-10 ps relative to that at its maximum value at ∼1 ps, for all of the pump-probe transients shown in Figures 4 and 5.[78] It is clear from Figure 6 that for the intermediate excitation wavelengths investigated, excitation of sodide in THF always produces the highest fraction of long-lived electrons whereas excitation of sodide in DG leads to the lowest fraction of long-lived electrons, with DME presenting an intermediate case. The magnitude of the difference in the fraction of long-lived electrons is more than could be explained by any small differences in the sodide CTTS absorption spectrum between these solvents.[79] Thus, since the data in Figures 4 and 5 show that the time scale for detached electrons to appear is the same in all the solvents studied here,[80] we expect that it is the number of solvent-supported disjoint electronic states available at the energy of the CTTS excitation that determines the number of long-lived electrons that remain following photodetachment

of electrons from sodide in the different solvents.

Based on the results of mixed quantum/classical simulations,[10,11,14,17] we expect that the probability that an excited CTTS electron will couple to a disjoint state is dictated both by the energy of the disjoint state (relative to the CTTS excited state) and the density of cavities in the solvent. The energy of the disjoint states is dominated by the size and electrostatic potential of the cavities; cavities that are large enough to hold an electron and are also electrostatically positive will serve as deeper traps. The density of the disjoint states is determined simply by the density of the cavities; a solvent with with more cavities has more disjoint states. Thus, we believe that it is the density of cavity-supported electronic states at the energies accessed by CTTS excitation of sodide at intermediate wavelengths that is responsible for the differences in the number of long-lived electrons in the different ethers: DG has the smallest density of disjoint states accessible by the CTTS excited electron and THF has the largest.

If it is really a difference in the density of disjoint states that causes the different relative number of long-lived electrons formed by photodetachment from sodide at intermediate excitation wavelengths in the different solvents, then why do the lowest (785 nm) and highest-energy (395 nm) excitation wavelengths still produce the same number of long-lived electrons in all of the solvents studied, as seen in Figure 4? For excitation on the high-energy side of the sodide CTTS band, we expect that photoexcitation provides direct access to the solvent-supported disjoint states[10,11,17] (or possibly even to the solvent conduction band[81,82]), so that the photodetachment process directly ejects electrons far into solution. At these high excitation energies, we expect the density of the disjoint states to be quite high,[10,14,17] so that in any of the solvents there is a significant number of states that can be accessed that eject an electron far into solution. Since the density of disjoint states is so high at these high excitation energies, any differences in the density of cavities in the different solvents that lead to different dynamics at intermediate excitation wavelengths is not as important. This causes the number of long-lived electrons to be the same in all the solvents for this high energy excitation.

For excitation on the low-energy side of the sodide absorption band, on the other hand, the fact that the number of long lived electrons is all the same is more difficult to understand. We expect that only a few of the most deeply-bound solvent-cavity-supported electronic (disjoint) states will be energetically and spatially available to couple to the localized, bound

CTTS excited state of the anion, as is observed by the fact that there are only a few long lived electrons for this excitation wavelength in all the solvents. The fact that we see similar recombination dynamics following 785-nm CTTS photodetachment from Na^- in the different ethers, however, indicates that solvent-supported disjoint states are equally accessed in these solvents. This suggests that the most deeply-bound cavity states 'turn on' at about the same energy in all of the ethers, although we do not fully understand the reason that these low-energy states are equally accessible while the intermediate disjoint states are not.

We have expressed this idea of the varying number of cavity-supported electronic states in the different solvents pictorially in Figure 7. In this figure, we represent the dipole-allowed sodide CTTS transitions as being from a ground *s*-like state to one of three quasi-degenerate bound excited states (purple lines).[40,44] Since we do produce a small number of long-lived electrons even with 785-nm excitation in all the solvents (Figure 4), we have drawn the figure so that the most deeply-bound solvent-supported disjoint states begin just below the 785-nm excitation energy. The density of solvent-supported states increases in each of the solvents at higher excitation energies, providing more possibilities for coupling between the bound CTTS excited states and disjoint states that can lead to electron relocalization at intermediate excitation wavelengths. We have used the level of color shading in Figure 7 to indicate the relative density of disjoint states; based on the data in Figure 6, we believe that the rate at which the density of disjoint states increases with energy is lower in DME and still lower in DG than it is in THF. At the highest excitation wavelengths, excitation is directly to the solvent-supported states,[83] so we believe that most of the excited electrons are relocalized far into the solvent and do not recombine on fast time scales.

C. The Effects of Bulk Solvent Properties on Long-Time Electron Recombination Dynamics

Another aspect of sodide CTTS-electron dynamics that we have explored is the rate at which the long-lived electrons undergo recombination in the different ether solvents. For photodetachment from sodide in THF, we have argued in previous work that the long-lived electrons fall into two distinct classes: those electrons that undergo recombination on a hundreds-of-picoseconds time scale, and the remainder that do not recombine on sub-ns time scales.[19,21,22,40–43,49] Since the recombination kinetics of those long-lived electrons

that do recombine are not diffusive, we referred to this class of electrons as being 'solvent separated', and we hypothesized that these electrons are likely localized only one or two solvent shells away from their neutral partners.[19,21,22,40–43,49] One of the features that led us to conclude that the recombination of solvent-separated electrons was not diffusive was that the recombination time scale depended on solvent polarity and not viscosity: we saw slower recombination times in more polar solvents.[40] In contrast, we referred to those electrons that do not recombine on sub-ns time scales as 'free electrons', and inferred that these electrons are ejected to distances that are quite far from their neutral parent atom.[19,21,22,40–43,49] In this subsection, we investigate how the long-time recombination dynamics of the photodetached electrons varies across our series of ether solvents.

In Figure 8 we show the long-time dynamics of the solvated electrons created via 395-nm photodetachment from sodide in the different ether solvents; the data in each solvent have been scaled to match at ∼6-9 ps and the y-axis in this figure has been expanded so that the long-time dynamics can be easily compared. The data show that the time scale for the long lived electrons to recombine depends significantly on the choice of solvent. A quick glance at Table I shows that this trend does not correlate with solvent viscosity, but instead better matches the solvent polarity as measured by the E_T^N values. Thus, the slow electron recombination dynamics in these solvents follows the trend seen previously,[40] with the rate of long-time electron recombination scaling roughly inversely with solvent polarity. We believe that the trend in the rate of solvent-separated electron recombination with solvent polarity is best explained by the idea that this back electron transfer reaction is in the Marcus inverted regime: the more polar the solvent, the greater the barrier to the back electron transfer and thus the smaller the rate.[40]

V. DYNAMICS OF THE NEUTRAL SODIUM SPECIES PRODUCED FOLLOWING CTTS PHOTODETACHMENT FROM SODIDE IN DIFFERENT ETHERS

Following CTTS photodetachment of the electron from sodide, the dynamics of the neutral sodium species that remains behind are quite complex, as summarized in the introduction and in Eq. 2. New insight into each of the processes in Eq. 2 has come from mixed quantum/classical molecular dynamics simulations, which show that the reaction of the

sodium atom to produce the TCP and the subsequent solvation of the TCP in liquid THF is driven almost entirely by the motion of just four first-shell solvent molecules.[69] The simulations suggest that the observed chemical reaction to produce the (Na^+, e^-) TCP from the neutral Na atom occurs oxygen sites on the closest one or two solvent molecules move close enough to coordinate with the cation end of the TCP, displacing the sodium atom's valence electron. The simulations also indicate that the remainder of the TCP solvation that occurs on a ∼5-10 ps time scale reflects the motion of oxygen sites on additional first-shell solvent molecules to create a tightly-knit, 4-site arrangement around the positive end of the TCP dipole.[69] In this section, we examine how the dynamics of both TCP formation and the subsequent TCP solvation varies across the series of ether solvents presented in Figure 1.

A. Solvent Independence of the Reaction of the Gas-Phase-Like Sodium Atom to Form (Na^+, e^-)

In Figure 9 we show the results of experiments where we excited the sodide CTTS transition at 395 nm and probed the initially-formed neutral sodium atom near its absorption maximum at 580 nm in our series of ether solvents. Since the electron dynamics (and therefore the Na^- bleach dynamics) are essentially identical in all the solvents for this excitation wavelength (see Figure 4), we do not have to worry about disentangling the bleach dynamics from the neutral sodium dynamics in any of the data presented here. Thus, any differences in the 580-nm spectral dynamics that we observe in the different solvents must be due to differences in the dynamics of the neutral sodium absorber; we do not need to assume a kinetic model[14,40,44] to compare the dynamics in different solvents. Figure 9 shows, however, that aside from a slight difference in THF, the dynamics of the initially-created neutral sodium atom is identical in all of the ether solvents.

In previous work,[14] we argued that the decay of the 580-nm absorption was almost entirely due to the chemical reaction that converts the neutral sodium atom into the (Na^+, e^-) TCP. Thus, the data in Figure 9 suggest that the ∼750-fs time scale for the reaction to form the unsolvated sodium atom tight-contact pair from the initially formed gas-phase-like sodium atom[14] is essentially solvent independent. This means that the rate-determining step in this reaction is independent of solvent viscosity; instead, it is dominated by local solvent motions. This observation is consistent with the mixed quantum-classical molecular

dynamics simulations, which suggest that the spectral dynamics at 580 nm is dominated by the time for the closest solvent molecule to reorient to bring one of its oxygen atoms close enough to coordinate with the sodium cation core of the neutral atom, driving the formation of the chemically distinct TCP species.[69] Simulations suggest that the solvent motions needed to bring an oxygen atom close to the neutral Na species should take place on about the same time scale for all the linear-chain ethers,[29] consistent with our observations. The fact that the interconversion time scale is slightly faster in the cyclic ether THF likely represents the fact that the THF ring can rotate more easily to bring its oxygen atom to bear on the neutral sodium atom than can the linear-chain ethers.

B. Solvent Dependence of the Solvation Dynamics of the (Na^+, e^-) TCP

In liquid THF, we saw in previous work that once the ∼750-fs chemical reaction to form the (Na^+,e^-)* TCP from the initially-created neutral sodium atom was complete, the newly-formed TCP takes ∼5-10 ps to equilibrate with the solvent.[14] The spectral signature of this equilibration was a red-shift in the absorption spectrum of the TCP, from ∼750 nm for the newly-crated (Na^+,e^-)* to ∼900 nm for the equilibrated solvated (Na^+, e^-) whose absorption spectrum is shown as the purple dashed curve in the lower panel of Figure 2. We found that this solvation-induced red-shift was most easily monitored via the rise in absorption intensity on the red edge of the TCP absorption band near ∼1100 nm, where the TCP has a reasonable cross section.[14,84]

To see how this solvation time scale changes in different solution environments, Figure 10 shows the results of experiments where we used 395-nm light to photodetach electrons via CTTS excitation of sodide and probed the dynamics of the neutral TCP species at 1110 nm in our series of ether solvents; the data in both panels have been scaled to unity at ∼25 ps so that the early-time dynamics in the different solvents can be easily compared. The instrument-limited rise seen at this wavelength represents the absorption of the initially-prepared CTTS excited state, and the slower ∼0.5-ps rise tracks the formation of the solvated electron and (Na^+, e^-) TCPs produced from partial electron ejection from the neutral sodium atom.[40] The subsequent small ∼1-ps decay tracks the loss of TCPs and solvated electrons due to the small amount of fast geminate recombination process seen at this excitation wavelength (*cf.* Figure 4),[41] and the final longer (∼5-10-ps) absorption rise cleanly tracks

the solvation of the remaining TCPs since all of the other processes are complete on this time scale.[14] The data in Fig. 10 show clearly that the TCP solvation dynamics measured at this wavelength are essentially identical in THF, DME, and DG.[85] The fact that this long solvation time scale is so similar in solvents with different viscosities suggests that like the sodium atom-TCP interconversion reaction, this longer-time solvation process also only involves local solvent motions and not long-ranged structural rearrangement. Thus, this observation is consistent with the picture developed by our simulations, which suggests that this long-time solvation involves only the motion of just a few molecules in the first solvent shell as they coordinate their oxygen sites with the cation end of the TCP.[69]

The fact that the time scale for the oxygen coordination of the cation end of the (Na^+, e^-) TCP is similar in THF, DME and DG may initially seem surprising, but this observation is also consistent with the results of classical molecular dynamics simulations. Olender *et al.* simulated the solvation of newly-created sodium cations in the $CH_3(CH_2OCH_2)_nH$ series of ether solvents (with n = 1, 2, and 4) and found that the solvation time scale, which involved 'chelation' of the cation by the ether oxygen sites, was essentially independent of the ether chain length.[29] These authors explained this result by arguing that the solvation dynamics they observed were dominated by local motions of the individual C-O-C links in the ether chains,[29] a mechanism similar to what we observe in our mixed quantum/classical simulations.[69] We note that the time scale observed for Na^+ solvation in the classical simulations in Ref. 29 was faster than that seen experimentally for the TCP in Figure 10. This is likely because these simulations did not account for the fact that sodium cations are much smaller than the neutral species from which they are created, and we have shown in previous work that the time scales for solvent relaxation when the solute size decreases are much longer than those accompanying simple changes in solute charge or dipole moment.[86,87] Thus, the fact that slow solvation dynamics of the (Na^+, e^-) TCP in the different ethers is so similar is supports our claim that the underlying solvent motions involve only a few first-shell molecules coordinating the cation end of the TCP.

Figure 10 also shows that although the long-time solvation dynamics of the (Na^+, e^-) are similar in THF, DME, and DG, the long-time solvation of the TCP is quite a bit faster in DEE than in the other solvents. The faster rise time seen at this probe wavelength suggests either that the mechanism by which the TCP is formed is different in DEE or that the nature of the equilibrated TCP is different in DEE than in the other ethers. We note the time scale

for the first solvent molecule to solvate the cation end of the TCP, which we associate with the reaction that produces the TCP from the neutral sodium atom, is the same in DEE as in the other ethers (*cf.* Fig. 9). We also note that the simulations of Olender *et al.* argued that the longer-time solvation processes of different ethers should also be similar. Thus, we believe that the nature of the TCP in DEE is different than that in the other ether solvents. DEE is the least polar of our solvent series, and one possibility is that the cation end of the equilibrated TCP in DEE is coordinated by fewer solvent oxygen atoms than in the other ethers; if this were the case, it could be that the TCP formed in DEE is less stable than the TCP formed in the other solvents. This idea could also explain why the equilibrated TCP is not observed in pulse radiolysis experiments in DEE:[73] less coordination of the TCP cation would make the TCP less stable relative to sodide. We plan to explore the nature of the TCP formed in DEE and its long-term stability in future work.

VI. CONCLUSIONS

In this paper, we have used the dynamics of electron photodetachment following CTTS excitation of sodide as a way to investigate the possible existence of naturally-occuring solvent cavities in the THF, DEE, DME and DG series of ethers. We found that the short-time dynamics of electron photodetachment from Na^- were identical in all of these solvents: following CTTS excitation, the photodetached electrons all appeared after a ∼0.5-ps delay with their equilibrium absorption spectrum, suggesting that the excited electrons are localized into pre-existing solvent traps. This suggests that DEE, DME and DG, like liquid THF, are solvents that naturally contain voids that can support low-lying disjoint electronic excited states.[10–12,12,14,17,18] We also found that the amount of fast geminate recombination of the detached electrons was the same in all the solvents following CTTS excitation of sodide at both 395 nm and 785 nm. The similarity seen in the different solvents with 785 nm excitation implies that the lowest cavity-supported electronic states turn on at about the same energy in each of these solvents, and that once a disjoint state is accessed, the physics of electron localization after an electron accesses a disjoint state is also roughly independent of solvent. We also saw, however, that for intermediate excitation wavelengths, the fraction of detached electrons that undergo fast geminate recombination was different in the different ethers. This suggests that the density of cavities is different in the different ethers, with the

longer-chained, more polar DG solvent containing fewer naturally-occuring cavities of the correct size and polarization to couple to the CTTS excited state than either liquid THF or the shorter-chained DME solvent. It would certainly be interesting to probe the differences in cavity density across this series of solvents using neutron diffraction and/or molecular dynamics simulation; differences in cavity density also might be revealed via scavenging experiments following the CTTS photodetachment of iodide to measure electron ejection distances in these solvents.[17]

We also examined the dynamics of the neutral sodium species that remains following CTTS photodetachment of an electron from sodide and found that the relaxation of this species was the same across our series of ether solvents: the reaction to form the (Na^+, e^-) from the initially-produced neutral sodium atom occurs at the same rate in DEE, DG and DME and is only slightly faster in THF. This suggests that only local solvent motions, such as the coordination of the closest solvent molecule's oxygen atom with the cation end of the TCP, and not bulk solvent rearrangements are what is responsible for driving this reaction. We also found that the slow solvation dynamics of the (Na^+, e^-) is nearly identical in THF, DME and DG, again pinpointing the important role of local solvent motions in this long-time solvation process. We did observe different long-time solvation dynamics of the TCP in DEE, where the faster time scale suggests that the nature of the TCP is different in this solvent than in the other ethers, possibly a result of DEE's low polarity. But the similarity of the solvation dynamics in DEE, DG and THF is consistent with the results of our mixed quantum/classical molecular dynamics simulations, which pinpoint the local interactions of only four first-shell solvent oxygen atoms with the positive end of the TCP dipole as the primary coordinate for solvation.[69]

The idea that only local solvent motions play a role also can explain why the linear response approximation fails to describe the solvation of the (Na^+, e^-) TCP:[51] since motions of only a few molecules are involved,[69] the corresponding fluctuations of those molecules is not Gaussian, and the motions of these molecules that equilibrate the TCP are different from their natural motions at equilibrium. Thus, the observation of similar long-time solvation time scales here strongly suggests that the linear response approximation would fail to describe the solvation of the TCP in the entire series of ethers;[51] such a breakdown of linear response also has been observed in the classical MD simulations of Olender *et al.*[29]

We close by commenting on the fact that essentially all of the short-time dynamics we

observe following CTTS photodetachment from sodide are identical in the different ethers, including the time scales for physical processes as varied as electron ejection, electron relocalization, TCP formation and geminate recombination. The fact that these time scales are so similar across our solvent series reinforces the idea that all of these processes are driven by local solvent motions, and that bulk solvent properties such as viscosity (with the exception of polarity in the case of the longer-time geminate recombination) play only a secondary role. Thus, the rates of the solvent-driven processes investigated here would not be well predicted by dielectric continuum or other simple theories that are based predominantly on bulk solvent parameters. We believe this is because most of the dynamics of electron photodetachment is determined by the presence of the naturally-occurring molecular-scale cavities in these liquids. Clearly, more work needs to be done to understand the driving force for the existence of cavities in the ethers and to determine how common cavities are in other families of solvents. Moreover, it is critical to incorporate the molecular aspects of cavities and the role they play in electron detachment and dynamic solvation into theories of solution-phase chemical reactivity if we are to gain a better understanding of the important chemical differences between cavity-containing and non-cavity-containins liquids.

Acknowledgements: This work was supported by the National Science Foundation under Grant Nos. CHE-0603766 and CHE-0908548. The authors thank Drs. Ross E. Larsen and Arthur E. Bragg for useful discussions.

FIG. 1: Molecular structure of the solvents studied in this work: tetrahydrofuran (THF), diethyl ether (DEE), 1,2-dimethoxyethane (DME), and diglyme (DG).

FIG. 2: Absorption spectra of sodide and the sodide CTTS photoproducts in the ethers shown in Figure 1. Upper Panel: Absorption spectra of sodide in THF (black curve), DEE (blue dotted curve), DME (green dot-dashed curve) and DG (red dashed curve) as measured in our laboratory; since we could not independently determine the concentration of our samples, we assumed each spectrum had the same maximum extinction coefficient as sodide in THF. The grey dashed curve shows the spectrum of sodide in THF taken from the Gaussian-Lorentzian parameters presented in the literature,[47] which should be free of spectral contributions from potasside and/or scattering. Lower Panel: Absorption spectra of the solvated electron in THF (black curve), DEE (blue dotted curve), DME (green dot-dashed curve) and DG (red dashed curve) taken from Gaussian-Lorentzian parameters given in the literature.[68] The thin purple dashed curve shows the absorption spectrum of the sodium cation:electron tight-contact pair, (Na^+, e^-), in THF, also taken from the literature.[47]

FIG. 3: Electron photodetachment dynamics following excitation at both the low-energy and high-energy sides of the CTTS band of sodide in both DME and DG. Upper Panels: Ultrafast absorption transients for sodide samples in DME (Left Panel) and DG (Right Panel) excited at 395 nm and probed at various wavelengths where the solvated electron absorbs in the near-IR. Lower Panel: Ultrafast absorption transients for sodide samples in DME (Left Panel) and DG (Right Panel) excited at 785 nm and probed at various wavelengths in the near-IR where the solvated electron absorbs. For ease of comparison, all the data have been normalized at the maximum transient absorbance. We note that the delayed appearance of the electron's absorption and the complete lack of solvation dynamics also was seen for following excitation of sodide in both DEE and THF at these wavelengths,[14,18] suggesting that all four ether solvents contain cavities. The slight difference in the 1735-nm probe dynamics for the 395-nm excitation of sodide in DG (purple curve, Upper Right Panel) is likely an artifact coming from the front cell wall of the sample.

FIG. 4: Solvent dependence of the electron photodetachment dynamics following CTTS excitation of sodide. Left Panel: Ultrafast absorption transients probing the solvated electron's absorption near 2 μm following CTTS excitation of sodide at 395 nm in THF (black curve), DEE (blue dotted curve), DME (green dot-dashed curve) and DG (red dashed curve). Right Panel: Ultrafast absorption transients probing the solvated electron's absorption near 2 μm following CTTS excitation of sodide at 785 nm in the same four solvents as in the left panel (same color scheme). Although the exact probe wavelength is slightly different in each of these scans, we know that the spectral dynamics of the detached electron are are independent of probe wavelength, as seen in both Figure 3 and References 14, 15, and 18. The data have been normalized at the maximum transient absorption for ease of comparison.

FIG. 5: Electron photodetachment dynamics probed at 2130 nm following CTTS photoexcitation of sodide in THF (black curves), DME (green dot-dashed curves) and DG (red dashed curves) at 490 nm (Upper Panel), 575 nm (Center Panel) and 635 nm (Lower Panel). We were unable to cleanly extract electron photodetachment dynamics for sodide excited at intermediate wavelengths in DEE due to potasside contamination.[77] The data in each panel have been normalized to the maximum transient absorbance for ease of comparison.

FIG. 6: Fraction of long-lived electrons produced following CTTS photodetachment from sodide for different excitation wavelengths. The fraction is determined by the number of electrons that remain ∼7-10 ps after photodetachment relative to the maximum number of electrons produced ∼1 ps after photoexcitation from the data in Figures 4 and 5. Data shown are for CTTS excitation of sodide in THF (black diamonds), DEE (blue inverted triangles), DME (green squares) and DG (red triangles).

FIG. 7: Energy level schematic illustrating our understanding of the relative positions of the localized sodide CTTS states and the disjoint states supported by the naturally-occurring solvent cavities in THF (left), DME (center) and DG (right). The average energies of the sodide CTTS ground and optically-allowed excited states are shown as the purple lines; the adjacent purple Gaussian distributions indicate the fact that these states are likely homogeneously broadened. The density of solvent-supported disjoint states in each liquid is portrayed as being proportional to the degree of color in the band: darker color indicates a higher density of disjoint states at a given energy.[14,17] The recombination dynamics for electrons photodetached from sodide suggest that the lowest solvent-supported states turn on at about the same energy in each solvent, but that the density of the solvent-supported states increases more rapidly in THF than in DME and much more rapidly than in DG.

FIG. 8: Long-time electron photodetachment dynamics probed at 2085 nm following CTTS excitation of sodide at 395 nm in THF (black curve), DEE (blue dotted curve), DME (green dot-dashed curve) and DG (red dashed curve). The data have been scaled to match the transient absorbance between ∼6 - ∼9 ps and the y-axis has been expanded for ease of comparison.

FIG. 9: Ultrafast dynamics of the initially-created neutral sodium species and sodide bleach probed at 580 nm produced following 395-nm CTTS excitation of sodide in THF (black curve), DEE (blue dotted curve), DME (green dot-dashed curve) and DG (red dashed curve). The data has been normalized at the maximum transient absorbance for ease of comparison.

FIG. 10: Longer-time solvation dynamics of the (Na^+, e^-) TCP probed at 1110 nm following 395-nm CTTS excitation of sodide in THF (black curves), DEE (blue dotted curves) DME (green dot-dashed curves) and DG (red dashed curves). The initial rise and decay of the transients reflects absorption from the CTTS excited state and the small amount of fast recombination dynamics that still takes place at this excitation wavelength; the solvation dynamics of the TCP are reflected in the slower, 5-10 ps rise of the transient absorption (see text for details).[84] The Upper Panel highlights the first ∼10 ps of the dynamics and the Lower Panel shows the dynamics out to ∼35 ps. The TCP solvation dynamics are essentially the same within error in THF, DME, and DG, but different (and much faster) in DEE. The data in both panels has been normalized at ∼25 ps for ease of comparison.

* Currently at Department of Chemistry, University of Colorado, Boulder

† Electronic address: schwartz@chem.ucla.edu

[1] M. Maroncelli, Journal of Molecular Liquids **57**, 1 (1993).

[2] A. Warsher and W. W. Parson, Annual Review of Physical Chemistry **42**, 279 (1991).

[3] R. M. Stratt and M. Maroncelli, Journal of Physical Chemistry **100**, 12981 (1996).

[4] L. Reynolds, J. A. Gardecki, S. J. V. Frankland, M. L. Horng, and M. Maroncelli, Journal of Physical Chemistry **100**, 10337 (1996).

[5] M. Glasbeek and H. Zhang, Chemical Reviews **104**, 1929 (2004).

[6] W. P. de Boeij, M. S. Pshenichnikov, and D. A. Wiersma, Annual Review of Physical Chemistry **49**, 99 (1998).

[7] M. J. Lang, X. J. Jordanides, X. Song, and G. R. Fleming, Journal of Chemical Physics **110**, 5884 (1999).

[8] G. R. Fleming and M. H. Cho, Annual Review of Physical Chemistry **47**, 109 (1996).

[9] B. J. Schwartz and P. J. Rossky, Journal Of Physical Chemistry **99**, 2953 (1995).

[10] M. J. Bedard-Hearn, R. E. Larsen, and B. J. Schwartz, Journal of Chemical Physics **122**, 134506 (2005).

[11] M. J. Bedard-Hearn, R. E. Larsen, and B. J. Schwartz, Journal of Chemical Physics **125**, 194509 (2006).

[12] D. T. Bowron, J. L. Finney, and A. K. Soper, Journal of the American Chemical Society **128**, 5119 (2006).

[13] W. Glover, R. Larsen, and B. Schwartz, In preparation (2009).

[14] M. C. Cavanagh, R. E. Larsen, and B. J. Schwartz, Journal of Physical Chemistry A **111**, 5144 (2007).

[15] I. B. Martini and B. J. Schwartz, Journal of Chemical Physics **121**, 374 (2004).

[16] A. E. Bragg and B. J. Schwartz, Journal of Physical Chemistry A **112**, 3530 (2008).

[17] A. E. Bragg and B. J. Schwartz, Journal of Physical Chemistry B **112**, 483 (2008).

[18] M. C. Cavanagh, R. M. Young, and B. J. Schwartz, Journal of Chemical Physics **129**, 1 (2008).

[19] I. B. Martini and B. J. Schwartz, Chemical Physics Letters **360**, 22 (2002).

[20] We note that due to experimental limitations, in Ref. 18 we were unable to verify that electrons

ejected from K^- in DEE appeared with their equilibrium spectrum. The single-wavelength detachment kinetics we did observe, however, were identical to those from Na^- in this same solvent.

[21] I. B. Martini, E. R. Barthel, and B. J. Schwartz, Science **293**, 462 (2001).

[22] I. B. Martini, E. R. Barthel, and B. J. Schwartz, Journal of the American Chemical Society **124**, 7622 (2002).

[23] I. B. Martini, E. R. Barthel, and B. J. Schwartz, Thirteenth International Conference on Ultrafast Phenomena. Technical Digest (TOPS Vol.72) pp. 95–6—xxxi+484 (2002).

[24] W. Drabowicz, Zeitschrift Fur Naturforschung Section A-A Journal Of Physical Sciences **45**, 1342 (1990).

[25] J. P. Bareman, R. I. Reid, A. N. Hrymak, and T. A. Kavassalis, Molecular Simulation **11**, 243 (1993).

[26] J. Helfrich and R. Hentschke, Macromolecules **28**, 3831 (1995).

[27] S. Girard and F. Muller-Plathe, Molecular Physics **101**, 779 (2003).

[28] R. Faller, H. Schmitz, O. Biermann, and F. Muller-Plathe, Journal Of Computational Chemistry **20**, 1009 (1999).

[29] R. Olender and A. Nitzan, Journal of Chemical Physics **102**, 7180 (1995).

[30] G. D. Smith and D. Bedrov, Journal Of Physical Chemistry A **105**, 1283 (2001).

[31] S. Neyertz and D. Brown, Journal Of Chemical Physics **102**, 9725 (1995).

[32] Q. Zhong and J. T. Fourkas, Journal Of Physical Chemistry B **112**, 8656 (2008).

[33] D. T. Bowron, J. L. Finney, and A. K. Soper, Journal of Physical Chemistry B **110**, 20235 (2006).

[34] J. A. Kloepfer, V. H. Vilchiz, V. A. Lenchenkov, and S. E. Bradforth, Chemical Physics Letters **298**, 120 (1998).

[35] J. A. Kloepfer, V. H. Vilchiz, V. A. Lenchenkov, A. C. Germaine, and S. E. Bradforth, Journal of Chemical Physics **113**, 6288 (2000).

[36] V. H. Vilchiz, J. A. Kloepfer, A. C. Germaine, V. A. Lenchenkov, and S. E. Bradforth, Journal of Physical Chemistry A **105**, 1711 (2001).

[37] A. C. Moskun, S. E. Bradforth, J. Thogersen, and S. Keiding, Journal of Physical Chemistry A **110**, 10947 (2006).

[38] V. H. Vilchiz, X. Y. Chen, J. A. Kloepfer, and S. E. Bradforth, Radiation Physics and Chemistry

72, 159 (2005).

[39] E. R. Barthel, I. B. Martini, and B. J. Schwartz, Journal of Chemical Physics **112**, 9433 (2000).

[40] E. R. Barthel, I. B. Martini, E. Keszei, and B. J. Schwartz, Journal of Chemical Physics **118**, 5916 (2003).

[41] E. R. Barthel and B. J. Schwartz, Chemical Physics Letters **375**, 435 (2003).

[42] I. B. Martini, E. R. Barthel, and B. J. Schwartz, Journal of Chemical Physics **113**, 11245 (2000).

[43] E. R. Barthel, I. B. Martini, and B. J. Schwartz, Journal of Physical Chemistry B **105**, 12230 (2001).

[44] O. Shoshana, J. L. P. Lustres, N. P. Ernsting, and S. Ruhman, Physical Chemistry Chemical Physics **8**, 2599 (2006).

[45] Z. H. Wang, O. Shoshana, B. X. Hou, and S. Ruhman, Journal of Physical Chemistry A **107**, 3009 (2003).

[46] O. Shoshanim and S. Ruhman, Journal Of Chemical Physics **129** (2008).

[47] W. A. Seddon, J. W. Fletcher, F. C. Sopchyshyn, and E. B. Selkirk, Canadian Journal of Chemistry-Revue Canadienne de Chimie **57**, 1792 (1979).

[48] W. A. Seddon and J. W. Fletcher, Journal of Physical Chemistry **84**, 1104 (1980).

[49] I. B. Martini, E. R. Barthel, and B. J. Schwartz, Pure and Applied Chemistry **76**, 1809 (2004).

[50] E. R. Barthel, I. B. Martini, E. Keszei, and B. J. Schwartz, in *Ultrafast Phenomena XII*, edited by M. Murnane, N. Scherer, J. Miller, and A. Weiner (Springer-Verlag (Berlin), 2003), p. 459.

[51] A. E. Bragg, M. C. Cavanagh, and B. J. Schwartz, Science **321**, 1817 (2008).

[52] M. T. Lok, J. L. Dye, and F. J. Tehan, Journal of Physical Chemistry **76**, 2975 (1972).

[53] J. L. Dye, M. G. Debacker, and V. A. Niceley, Journal of the American Chemical Society **92**, 5226 (1970).

[54] J. L. Dye, Journal of Physical Chemistry **84**, 1084 (1980).

[55] J. L. Dye, Angewandte Chemie, International Edition **18**, 587 (1979).

[56] J. L. Dye, Progress in Inorganic Chemistry **32**, 327 (1984).

[57] This decrease in optical density likely results from reactions of Na^- with small amounts of impurities in the solvents or small amounts of air leaking into the cell. The OD decay typically occurred on a time scale of days and did not affect the dynamics in our pump/probe experiments within the 95% error bars shown in all the figures. We did not use data from a few samples whose optical density decay occurred on a time scale comparable to that over which we needed

to signal-average.

[58] T. Q. Nguyen, I. B. Martini, J. Liu, and B. J. Schwartz, Journal of Physical Chemistry B **104**, 237 (2000).

[59] S. Budavari, ed., *The Merck Index, Twelfth Edition* (Merck & Co. Inc, 1996).

[60] C. Laurence, P. Nicolet, M. T. Dalati, J. L. M. Abboud, and R. Notario, Journal of Physical Chemistry **98**, 5807 (1994).

[61] C. Carvajal, K. J. Tolle, J. Smid, and M. Szwarc, Journal Of The American Chemical Society **87**, 5548 (1965).

[62] To the best of our knowledge, the dielectric constant for DG has not been measured.

[63] D. R. Lide, ed., *CRC Handbook of Chemistry and Physics 88th Ed.* (CRC Press: Boca Raton, Fl, 2007), chap. Viscosity of Liquids, pp. 6–175–6–179.

[64] A. Pal and Y. P. Singh, Journal Of Chemical And Engineering Data **41**, 1008 (1996).

[65] C. Reichardt, Chemical Reviews **94**, 2319 (1994).

[66] This so-called E_T^N value of each solvent is based on a scale in which tetramethylsilane is defined to have an E_T^N value of 0 and water is defined to have an E_T^N value of 1.

[67] The absorption spectra of the solvated alkali anions, the solvated alkali atoms, and the solvated electron in THF have been shown to fit very well on the high energy side to a Gaussian and on the low energy side to a Lorentzian[47].

[68] F. Y. Jou and L. M. Dorfman, Journal of Chemical Physics **58**, 4715 (1973).

[69] W. Glover, R. Larsen, and B. Schwartz, In preparation (2009).

[70] R. Catterall, J. Slater, and M. C. R. Symons, Canadian Journal of Chemistry-Revue Canadienne de Chimie **55**, 1979 (1977).

[71] W. A. Seddon, J. W. Fletcher, and R. Catterall, Canadian Journal of Chemistry-Revue Canadienne de Chimie **55**, 2017 (1977).

[72] B. Bockrath and L. M. Dorfman, Journal of Physical Chemistry **77**, 1002 (1973).

[73] J. W. Fletcher and W. A. Seddon, Journal of Physical Chemistry **79**, 3055 (1975).

[74] W. A. Seddon, J. W. Fletcher, F. C. Sopchyshyn, and R. Catterall, Canadian Journal of Chemistry-Revue Canadienne de Chimie **55**, 3356 (1977).

[75] W. A. Seddon, J. W. Fletcher, R. Catterall, and F. C. Sopchyshyn, Chemical Physics Letters **48**, 584 (1977).

[76] Even though the LCP is not observed in equilibrium in liquid THF at room temperature,

we have found that if the temperature is decreased to ∼-60^{o}C, the LCP is produced in pulse radiolysis experiments, apparently in equilibrium with the TCP; M. C. Cavanagh-Larsen, J. R. Miller and B. J. Schwartz, unpublished results.

[77] As described in Ref. 18, we are unable to explore the disjoint state coupling in DEE for excitation wavelengths other than 395 nm or 785 nm due to possible interference from K^- contamination.

[78] The data in Figure 6 also were averaged over several different experiments and/or several different samples. Our choice of long-time scaling for calculating the fraction of long-lived electrons is justified since the appearance kinetics of the detached electrons is the same for all the solvents at all the excitation wavelengths investigated.

[79] In order to explain the difference in the fraction of long-lived electrons in different solvents from differences in absorption, the CTTS band of sodide in DG and DME would have to be shifted by ∼2700 cm^{-1} and ∼1500 cm^{-1}, respectively, relative to that in THF; instead, the experimental absorption spectrum of sodide in DG and DME are shifted by ∼700 cm^{-1} and ∼400 cm^{-1}, respectively, relative to that in THF (Figure 2).

[80] Although it is possible that there are differences in the electron absorption rise time in the different solvents that are too subtle for us to observe at the time resolution of our apparatus, we note that the difference in the number of long-lived electrons in DG relative to that in THF is as much as ∼50%, so that the corresponding ∼50% difference in electron appearance time would have been easily observed with our instrument.

[81] R. Lian, D. A. Oulianov, R. A. Crowell, I. A. Shkrob, X. Y. Chen, and S. E. Bradforth, Journal of Physical Chemistry A **110**, 9071 (2006).

[82] X. Chen and S. E. Bradforth, Annual Review of Physical Chemistry **59**, 203 (2008).

[83] There is also a probability that electrons excited to this highest energy could also be excited directly to a disjoint state. This could explain why all the dynamics at this high energy excitation are so similar in all the solvents.

[84] We note that this relatively slow solvation process occurs on a much different time scale than both the fast and the slow recombination dynamics. Thus, when probed near 1100 nm, this process is not masked by the changing population of TCPs (which amounts to ∼10% over the first ∼30 ps for the 395-nm excitation wavelength) and can be easily observed in the raw data.

[85] The small difference in the early-time dynamics of DG may be due to a small difference in the relative extinction coefficients of the (Na^+, e^-) and solvated electron at this probe wavelength

in this solvent.

[86] V. Tran and B. J. Schwartz, Journal Of Physical Chemistry B **103**, 5570 (1999).

[87] D. Aherne, V. Tran, and B. J. Schwartz, Journal Of Physical Chemistry B **104**, 5382 (2000).

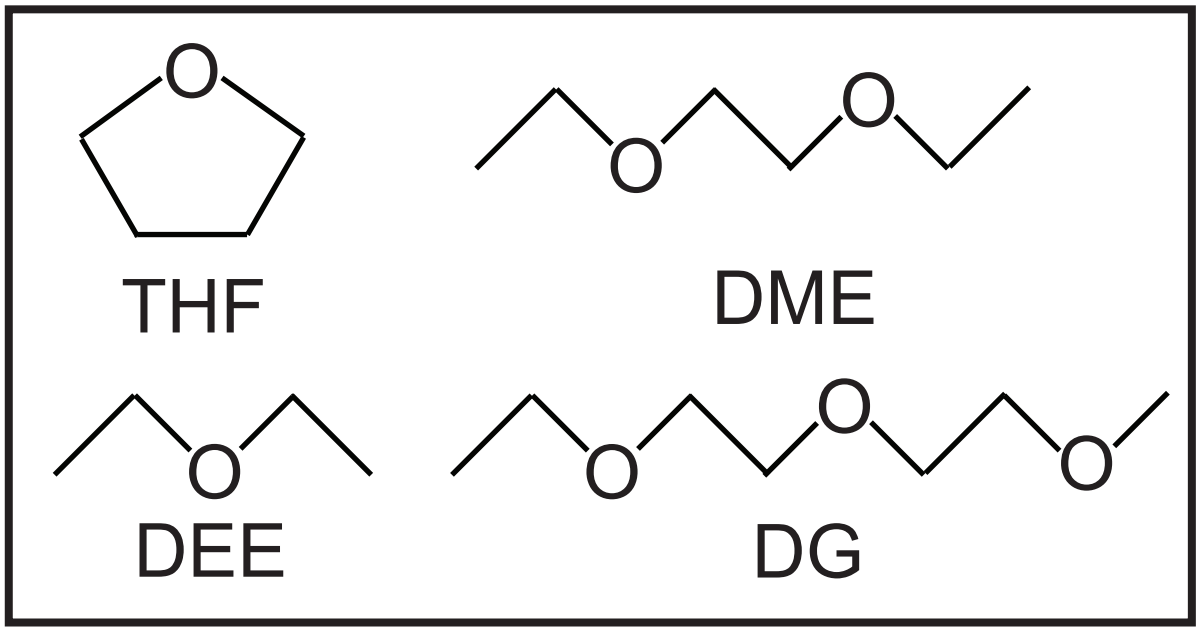

Cavanagh & Schwartz, Figure 1

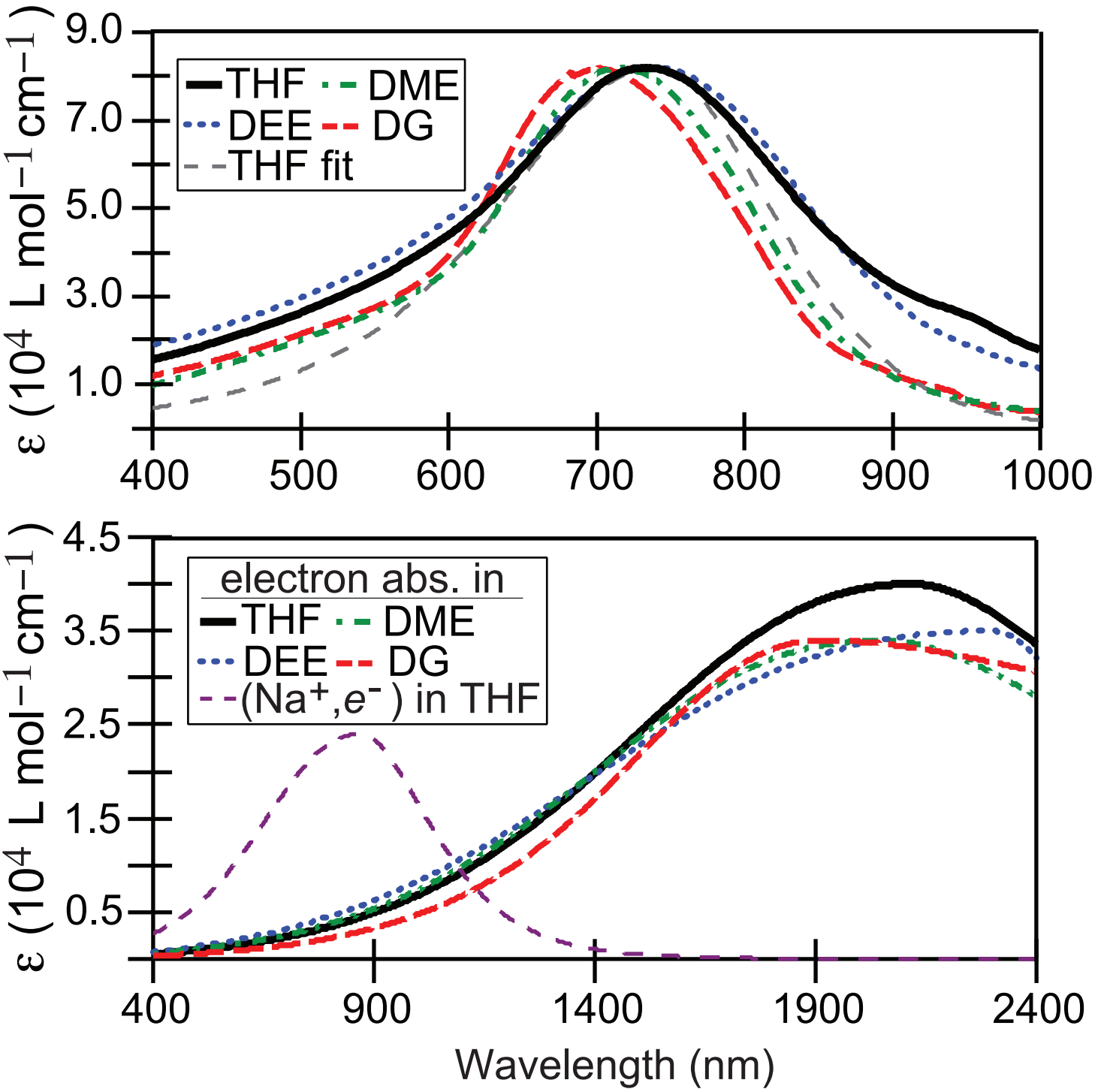

Cavanagh & Schwartz, Figure 2

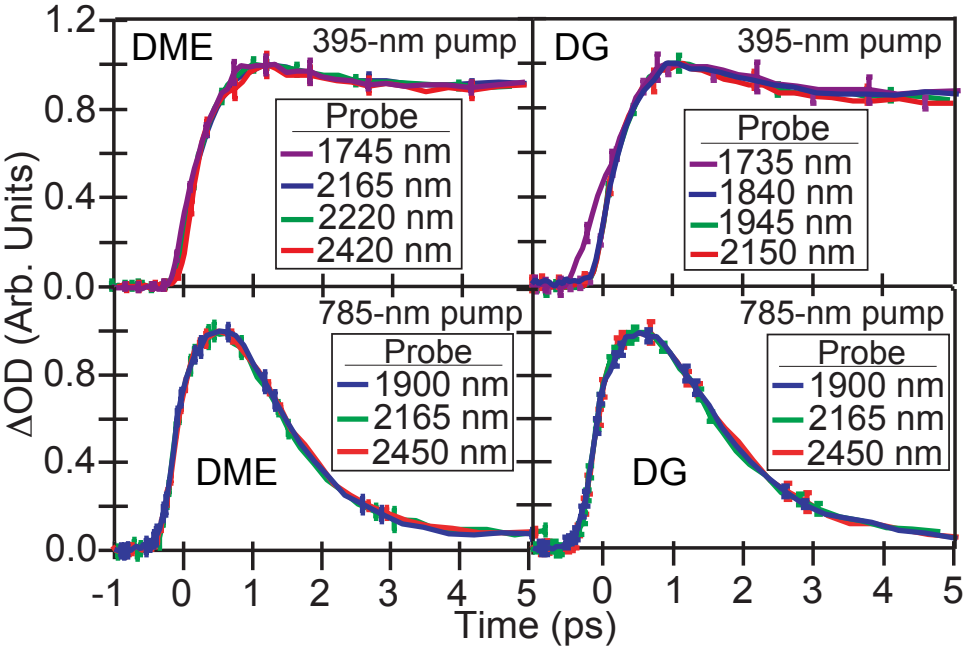

Cavanagh & Schwartz, Figure 3

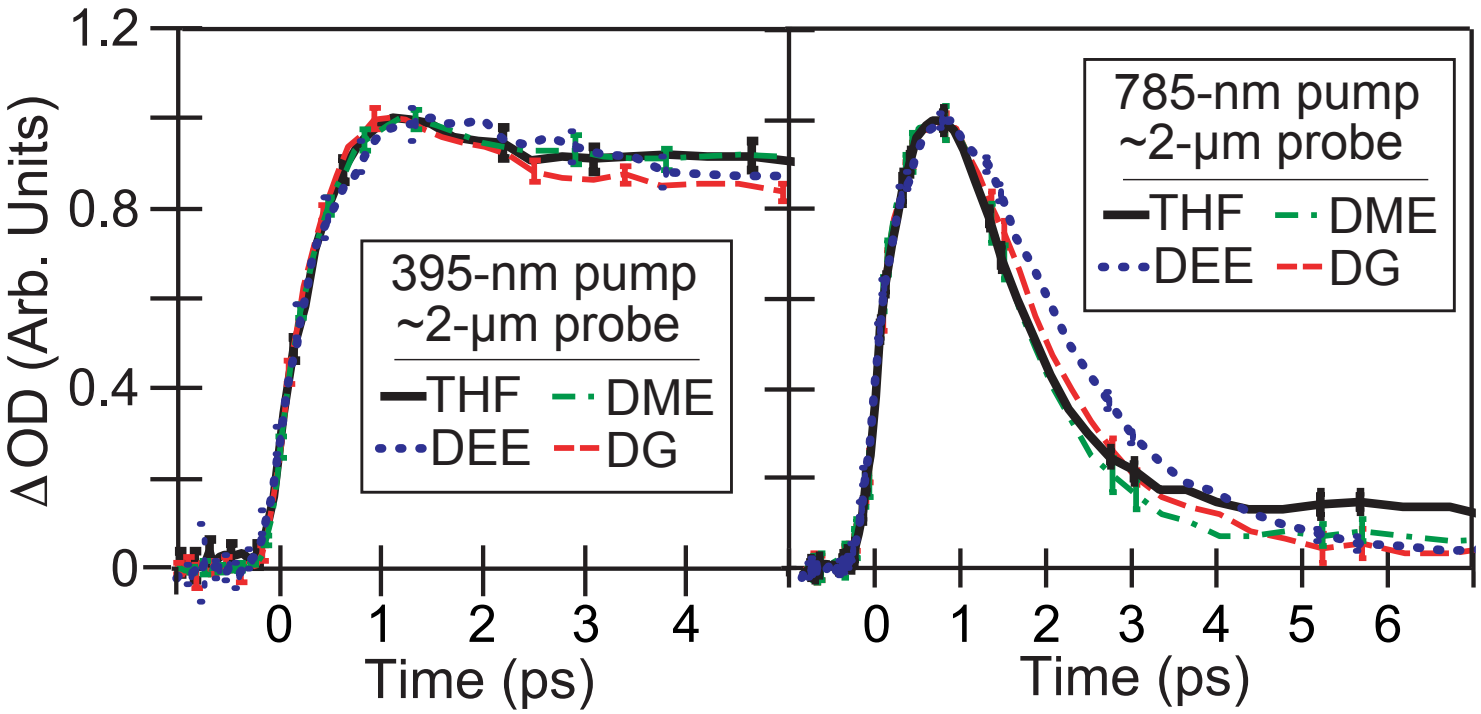

Cavanagh & Schwartz, Figure 4

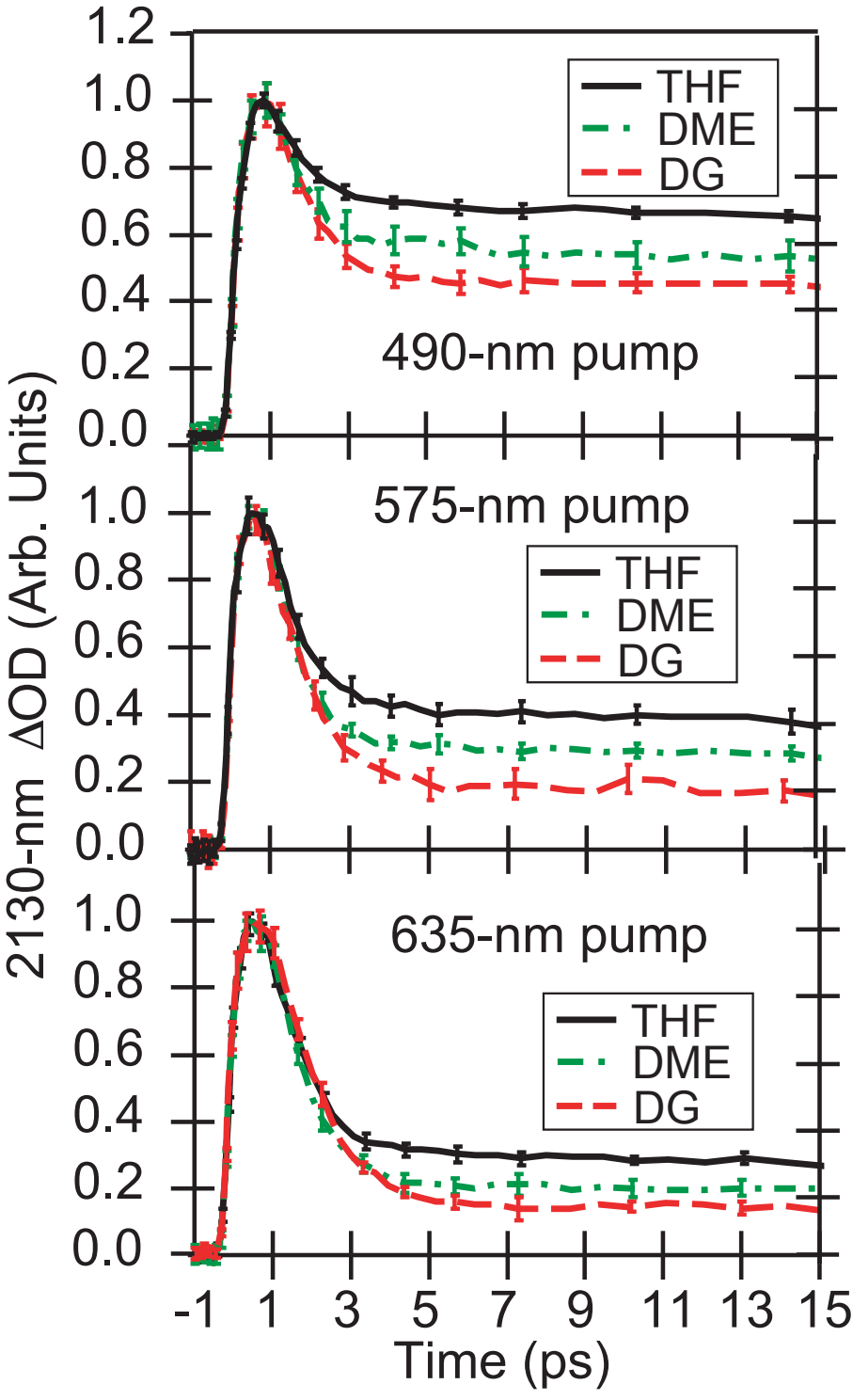

Cavanagh & Schwartz, Figure 5

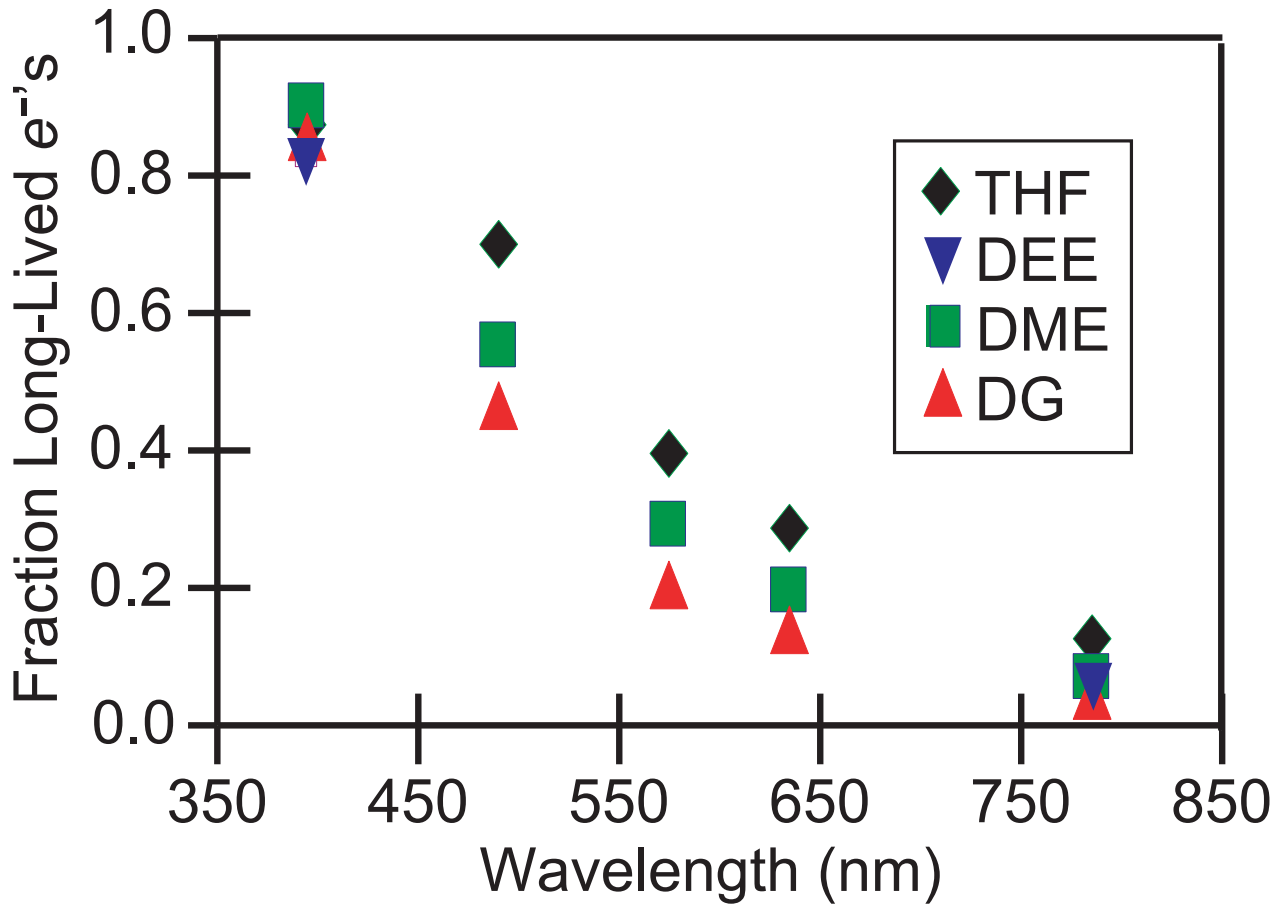

Cavanagh & Schwartz, Figure 6

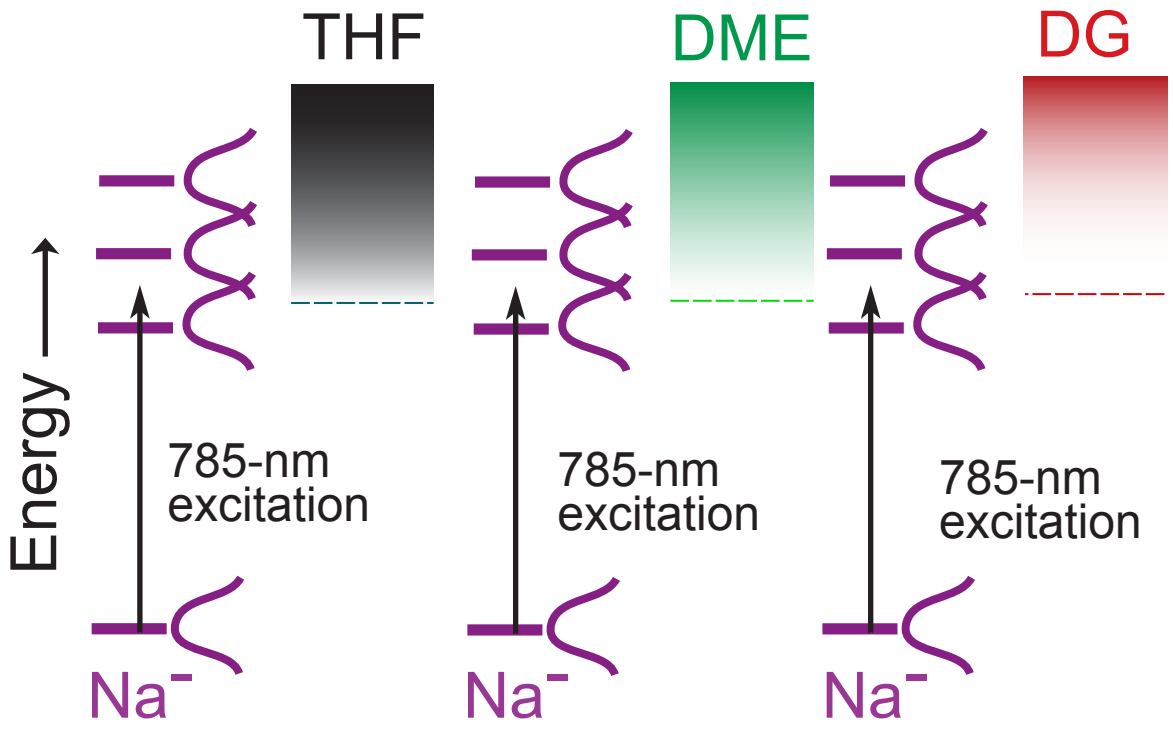

Cavanagh & Schwartz, Figure 7

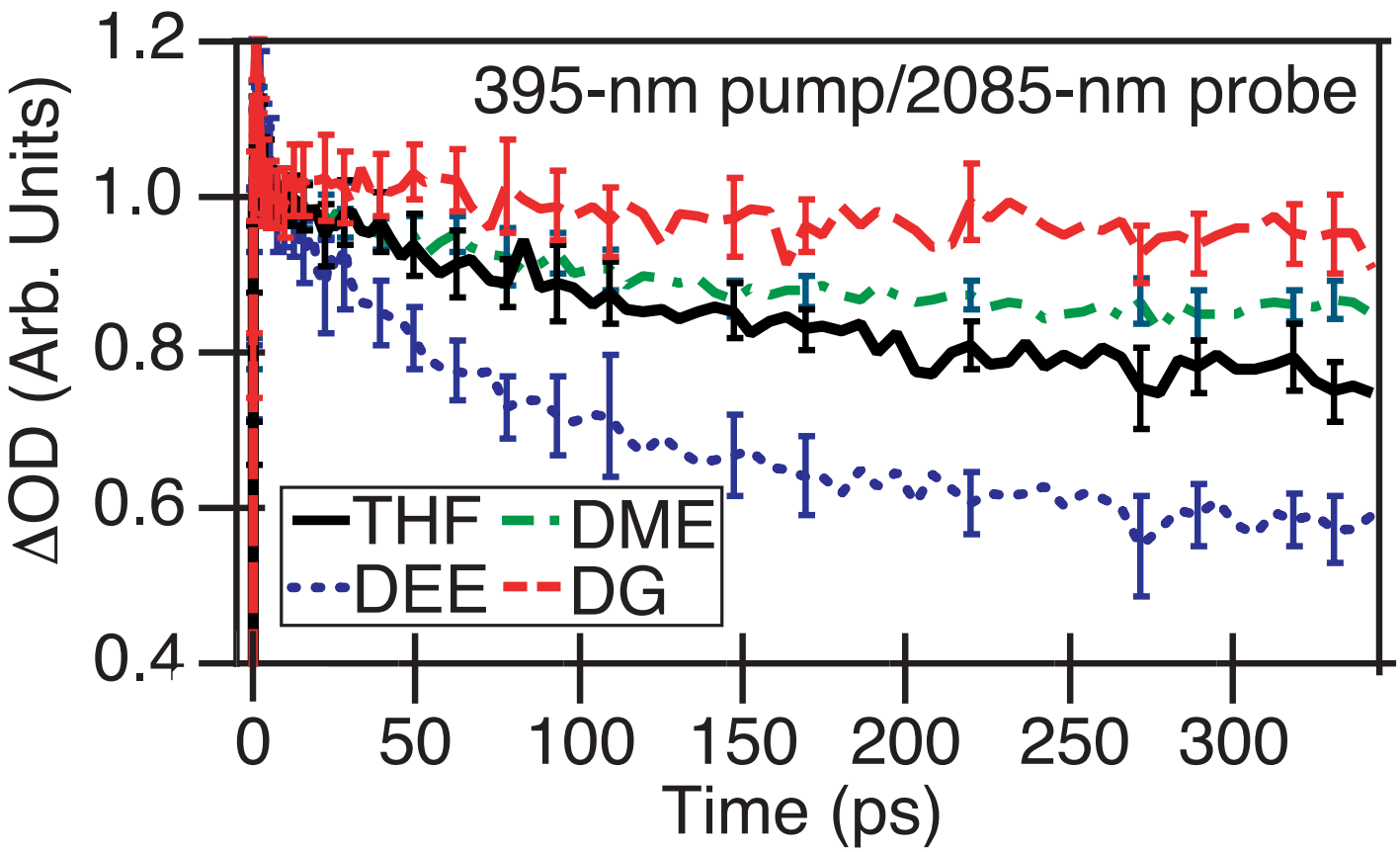

Cavanagh & Schwartz, Figure 8

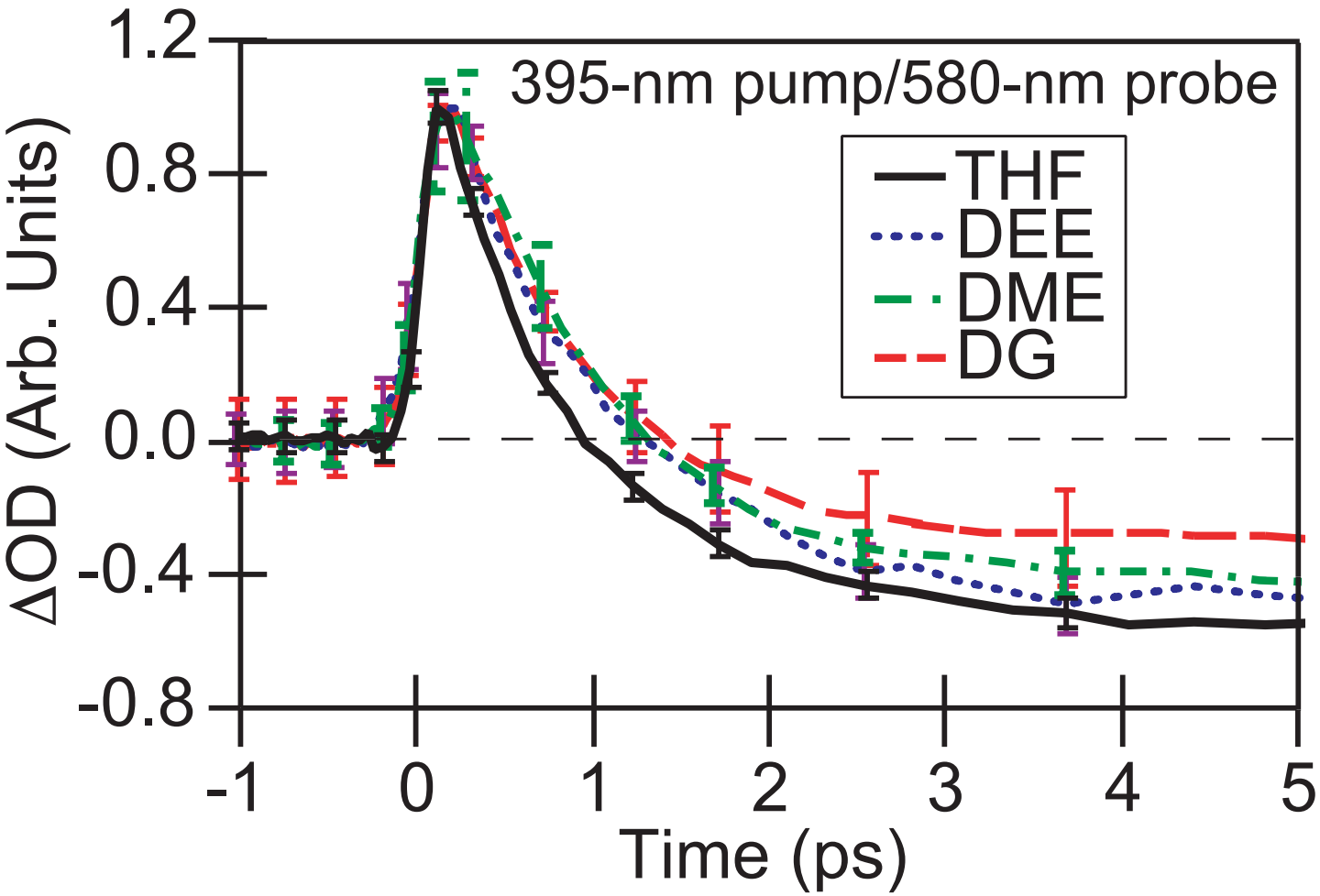

Cavanagh & Schwartz, Figure 9

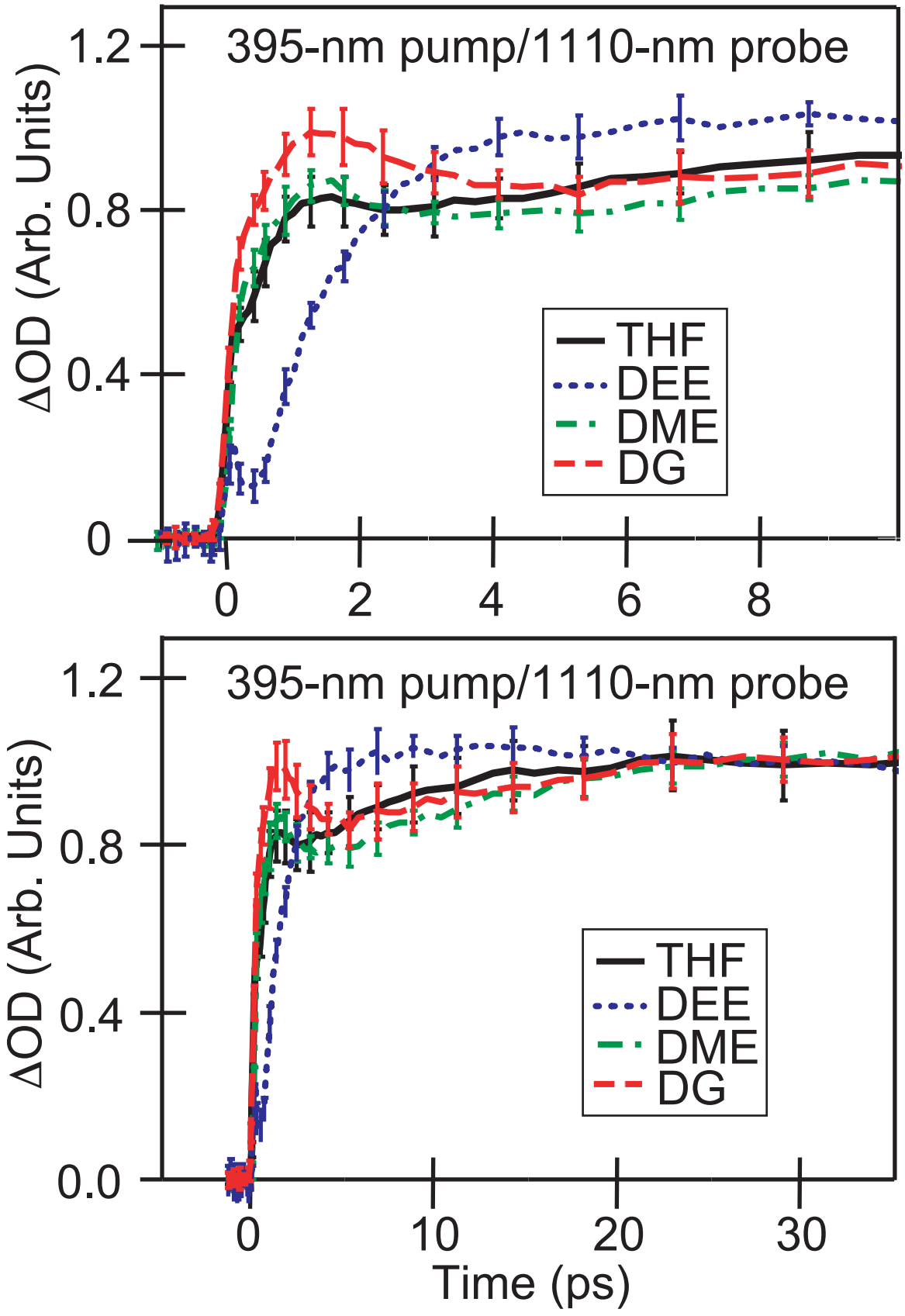

Cavanagh & Schwartz, Figure 10